



## First Evidence of Shape Coexistence in the $^{78}\text{Ni}$ Region: Intruder $0_2^+$ State in $^{80}\text{Ge}$

A. Gottardo,<sup>1,\*</sup> D. Verney,<sup>1</sup> C. Delafosse,<sup>1</sup> F. Ibrahim,<sup>1</sup> B. Roussière,<sup>1</sup> C. Sotty,<sup>2</sup> S. Rocca,<sup>3</sup> C. Andreoiu,<sup>4</sup> C. Costache,<sup>2</sup> M.-C. Delattre,<sup>1</sup> I. Deloncle,<sup>3</sup> A. Etilé,<sup>5</sup> S. Franchoo,<sup>1</sup> C. Gaulard,<sup>3</sup> J. Guillot,<sup>1</sup> M. Lebois,<sup>1</sup> M. MacCormick,<sup>1</sup> N. Marginean,<sup>2</sup> R. Marginean,<sup>2</sup> I. Matea,<sup>1</sup> C. Mihai,<sup>2</sup> I. Mitu,<sup>2</sup> L. Olivier,<sup>1</sup> C. Portail,<sup>1</sup> L. Qi,<sup>1</sup> L. Stan,<sup>2</sup> D. Testov,<sup>6,7</sup> J. Wilson,<sup>1</sup> and D. T. Yordanov<sup>1</sup>

<sup>1</sup>*Institut de Physique Nucléaire, CNRS-IN2P3, Université Paris-Sud, Université Paris-Saclay, 91406 Orsay Cedex, France*

<sup>2</sup>*Horia Hulubei National Institute for Physics and Nuclear Engineering, Bucharest-Măgurele, Romania*

<sup>3</sup>*CSNSM, CNRS-IN2P3, Université Paris-Sud, Université Paris-Saclay, 91406 Orsay Cedex, France*

<sup>4</sup>*Department of Chemistry, Simon Fraser University, Burnaby, British Columbia V5A 516, Canada*

<sup>5</sup>*University of Helsinki, Helsinki, Finland*

<sup>6</sup>*Istituto Nazionale di Fisica Nucleare, Laboratori Nazionali di Legnaro, 35020 Legnaro, Italy*

<sup>7</sup>*Flerov Laboratory of Nuclear Reactions, Joint Institute for Nuclear Research, Dubna, Russia*

(Received 26 January 2016; published 5 May 2016)

The  $N = 48$   $^{80}\text{Ge}$  nucleus is studied by means of  $\beta$ -delayed electron-conversion spectroscopy at ALTO. The radioactive  $^{80}\text{Ga}$  beam is produced through the isotope separation on line photofission technique and collected on a movable tape for the measurement of  $\gamma$  and  $e^-$  emission following  $\beta$  decay. An electric monopole  $E0$  transition, which points to a 639(1) keV intruder  $0_2^+$  state, is observed for the first time. This new state is lower than the  $2_1^+$  level in  $^{80}\text{Ge}$ , and provides evidence of shape coexistence close to one of the most neutron-rich doubly magic nuclei discovered so far,  $^{78}\text{Ni}$ . This result is compared with theoretical estimates, helping to explain the role of monopole and quadrupole forces in the weakening of the  $N = 50$  gap at  $Z = 32$ . The evolution of intruder  $0_2^+$  states towards  $^{78}\text{Ni}$  is discussed.

DOI: 10.1103/PhysRevLett.116.182501

The appearance of a well-defined shape in mesoscopic systems is linked to the existence of shell gaps, which helps to stabilize a given configuration by requiring a large energy to break it [1]. From this point of view, atomic nuclei represent a peculiar subset among finite many-body systems. In fact, even though nuclei show strong shell-closure effects, their energy gaps are the result of the interplay between single-particle structure (spherical energy levels) and collective excitations. These collective excitations can change or even overturn the spherical mean-field structure, as in the case of the “islands of inversion” [2]. Indeed, the coexistence of several shapes in nuclei is made possible by collective correlations bringing different configurations near in energy. A similar situation is also found in some metallic clusters, where shape isomers come close to the energy minimum [3]. In nuclei, there can be “intruder” configurations, different from the ground state, which have their origin in the excitation of nucleons to the higher-lying major shell. Their energy can be close to the ground state one, leading to shape coexistence. In particular, intruder  $0^+$  states which are two-particle two-hole ( $2p - 2h$ ) excitations in nature have their energy determined by the same forces changing the correlated shell gaps [1]. Therefore, they are an effective tool to investigate the interplay between shape coexistence and the spherical mean field.

A paradigmatic case in which the study of  $(2p - 2h)$   $0^+$  states can help to understand the shell-gap evolution is the

issue of the persistency of  $N = 50$  shell closure in neutron-rich systems. Recent experimental studies have pointed out a weakening of this gap at  $Z = 32$  [4,5]. This has led to speculations about a partial quenching of the shell gap going towards  $^{78}\text{Ni}$ , but subsequent mass measurements showed it is increasing again at  $Z = 30$  [6]. One hypothesis is that this behavior, instead of being an indication of a change in the single-particle energy, is due to the action of the quadrupole correlations, and so the stability of the spherical  $N = 50$  gap remains an open question [7,8]. A study of shape coexistence in this region will help disentangle the single-particle gap quenching from the effect of quadrupole collectivity across  $N = 50$ . This gap is of paramount importance for nuclear structure, being linked to fundamental issues such as the role of the three-body forces in the appearance of the spin-orbit shell closures [7,9].

The occurrence of shape coexistence near or at shell closures has been observed in many regions of the nuclide chart, from  $^{16}\text{O}$  [10] to  $^{182,184}\text{Hg}$  [11] and  $^{196}\text{Pb}$  [12]. This work provides the first evidence of shape coexistence close to  $N = 50$  and to  $Z = 28$ , following previous indications of low-energy intruder configurations at  $N = 49$  [13–16]. After the description of the experimental setup, the results of the measurement will be presented and discussed. It will be shown how the  $(2p - 2h)$   $0_2^+$  state in  $^{80}\text{Ge}$  gives a fundamental insight into the observed  $N = 50$  gap weakening at  $Z = 32$ , highlighting the mechanism involved.

The implications for shape coexistence on  $^{78}\text{Ni}$  will also be pointed out.

A radioactive low-energy  $^{80}\text{Ga}$  ion beam was produced in the photofission isotope separation on line (ISOL) facility ALTO, operated by the IPN in Orsay [17]. The ISOL target, a carburized mixture of uranium oxide and carbon nanotube powders [18], was placed in a Ta oven heated at 2000 °C. It was irradiated by a 50 MeV electron ( $e^-$ ) beam delivered by the ALTO linear accelerator, with an average beam current of 8  $\mu\text{A}$ . The single-charged surface-ionized reaction products were accelerated to 30 keV. The Production d'Atomes Radioactifs Riches en Neutrons (PARRNe) mass-separator magnetic field was set for mass 80. Previous studies show that the dominant production at this mass is  $^{80}\text{Ga}$  [19], due to its lower ionization potential compared to the neighboring isobars.

The mass-separated beam was then delivered to the experimental setup, consisting of a tape station with two measurement points. The first one, at the beam implantation point, was equipped with a plastic  $\beta$  detector and a coaxial high-purity Ge (HPGe) crystal for  $\gamma$  rays, to monitor the beam activity.

The  $^{80}\text{Ga}$  yield was measured to be  $\sim 10^4$  pps. Ions were collected on tape for 5 s, corresponding to several times the  $^{80}\text{Ga}$  half-life emissions of 1.9(1) and 1.3(2) s, belonging to the  $6^-$  ground state and to the  $3^-$  isomer, respectively [19].

The tape then moved the activity in about 1 s to the second measurement point: this was equipped with a plastic scintillator for  $\beta$  electrons, a coaxial large-volume HPGe crystal, and a liquid-nitrogen cooled Si(Li) junction for the detection of the conversion  $e^-$  (3 mm thickness). The three detectors were arranged as in Fig. 1. The efficiency of the  $\beta$  scintillator was about 20%, while the Ge crystal had a  $\gamma$ -ray efficiency of 0.7% at 1 MeV. The efficiency of the Si(Li) detector was 14%, measured for the 648 keV  $K e^-$  coming from the conversion of the 659 keV deexcitation of the  $2^+$  state of the daughter nucleus  $^{80}\text{Ge}$ , considering the 11.1 keV binding energy of the  $K e^-$  in Ge isotopes.

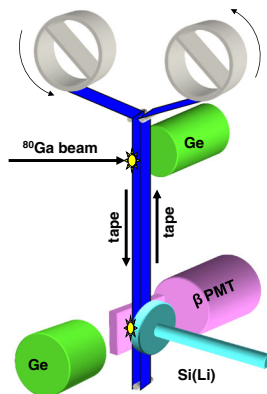


FIG. 1. Schematic view of the experimental setup. The tape moves the collected radioactivity in front of the Si(Li) detector.

All the internal conversion coefficients in this Letter were estimated on the basis of Ref. [20]. Data were acquired in a triggerless mode, with a 5 s acquisition time at each tape cycle. The beam purity was checked by measuring the  $\beta$ -delayed  $\gamma$  emission, previously studied in detail in Refs. [13,19]. The use of conversion  $e^-$  spectroscopy with ISOL beams has already been proven to be an effective tool to study excited  $0^+$  states by observing their  $E0$  decay to the ground state, as in the case of  $^{30}\text{Mg}$  [21]. Electron spectroscopy was not performed in the previous  $^{80}\text{Ga}$  studies in Refs. [13,19].

The  $\beta$ -gated  $e^-$  spectrum obtained from the Si(Li) detector can be seen in Fig. 2. The large background is due to the Compton edge at  $\sim 800$  keV, which originates from the 1080 and 1109 keV transitions in  $^{80}\text{Ge}$ , as well as from other higher-energy  $\gamma$  rays from the  $^{80}\text{Ga}$  decay observable in the spectrum. Two peaks appear clearly in the spectrum: the line at 648(1) keV is the aforementioned  $K e^-$  from the  $2^+ \rightarrow 0^+$  transition in  $^{80}\text{Ge}$ , while the other line at 628(1) keV does not correspond to any known transition in  $^{80}\text{Ge}$  or in any of its descendants. Moreover, there is no intense transition in the  $\gamma$  spectrum that could justify  $e^-$  conversion at 628 keV. This suggests that it is an  $E0$  transition associated with a second  $0^+$  state in  $^{80}\text{Ge}$ .  $\beta$  decay has already proven capable of populating low-lying  $0^+$  states in the region: in  $^{72}\text{Ge}$  a low-lying  $0_2^+$  state was found at 691 keV via its  $E0$  transition to the ground state [22]. It is noted that the spin-parity of the decaying  $^{72}\text{Ga}$  is  $3^-$ , as is the case for one of the two  $\beta$ -decaying states in  $^{80}\text{Ga}$  [19].

In order to verify this assignment, the time distribution of the 628 keV peak in the 5 s acquisition time was studied, and is shown in the inset of Fig. 2. The analysis yields  $t_{1/2} = 1.5(8)$  s for the 639(1) keV  $0_2^+$  state, which is compatible with the short  $^{80}\text{Ga}$  lifetimes, and incompatible with the longer decays of the daughter nuclei.

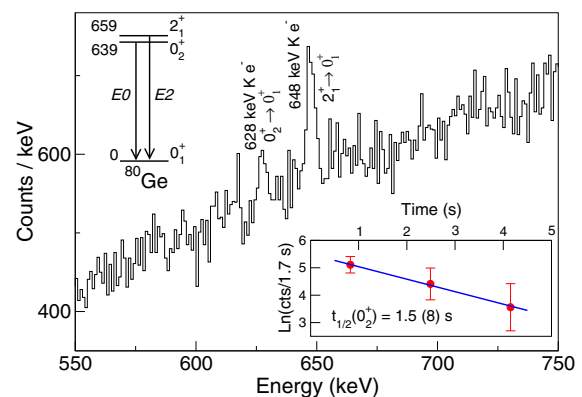


FIG. 2. Energy spectrum obtained from the Si(Li) detector from the decay of  $^{80}\text{Ga}$ . The inset shows the decay curve of the 628 keV  $e^-$ , which is compatible with the  $^{80}\text{Ga}$  lifetime(s). The deduced partial level scheme of  $^{80}\text{Ge}$  is also drawn.

In view of the large statistics and beam purity of the present experiment, it is worth investigating the possible  $\gamma - e^-$  coincidences. The upper panel of Fig. 3 shows the only peak clearly in coincidence with the 628 keV  $e^-$  line in the  $e^-$ -gated  $\gamma$  spectrum of the Ge crystal (without a coincident  $\beta$  condition to improve statistics). It is a  $\gamma$  ray at 1764(1) keV, previously undetected. The inset in the upper panel shows the 1764 keV gated Si(Li) spectrum, with the  $\beta$  condition applied: the 628 keV line stands out clearly. The lower panel of Fig. 3 presents the  $\beta$ -gated  $\gamma$  spectrum in the same energy region. The transition at 1773 keV in  $^{80}\text{Ge}$  was identified previously in Ref. [13], with an intensity of 1.3%. Relative to this level, the 1764 keV transition has an intensity of 0.4%, close to the observational limits of previous studies [13,19]. The inset in the lower panel of Fig. 3 shows the time distribution of this  $\gamma$  ray, yielding a half life of 1.6(4) s for the state feeding the  $0_2^+$  level, once again in agreement with the  $^{80}\text{Ga}$  half life, and incompatible with the longer ones of the descendants. A similar value is obtained for the decay curve of the  $\gamma$  rays in coincidence with the 628 keV  $e^-$ , thereby also confirming the decay curve of the  $e^-$  emission. If this transition directly feeds the  $0_2^+$  state, then there is a level at  $639 + 1764 = 2403(1)$  keV. Considering the decay properties of the  $3^-$  isomeric state in  $^{80}\text{Ga}$  [19], the spin-parity of this state is tentatively assigned as  $2^+$ , populated by first-forbidden  $\beta$  decay. This state has no isomeric character, being thus compatible with an  $E2$  transition to the  $0_2^+$  level or to some unobserved intermediate state. In conclusion, the present study indicates the existence of a 639(1) keV  $0_2^+$  state lower than the 659 keV first  $2^+$  level in  $^{80}\text{Ge}$ .

Shape coexistence in the  $Z = 40$ ,  $N = 50$   $^{90}\text{Zr}$  nucleus has been studied previously [23,24]. The  $\pi(2p - 2h)$  excitations across the  $Z = 40$  shell closure were suggested to be key to understanding it, while the  $\nu(2p - 2h)$  states

should be high in energy due to the reduced quadrupole interaction at  $Z = 40$  [25].

Given these premises, one can investigate what happens to  $\nu(2p - 2h)$  intruder configurations across  $N = 50$ , in the open proton  $fp$  shell between  $Z = 28$  and  $Z = 40$ , notably at  $Z = 32$ . Indeed, a substantial reduction of the excitation energy of the intruder  $\nu(2p - 2h)$   $0^+$  state is expected due to significant quadrupole interactions with the open-shell protons, on top of the gain in the pairing energy [1]. Moreover, the spherical mean field energies will be affected by the angular-momentum average of the residual interaction among valence nucleons [26]. This monopole drift will reduce the  $N = 50$  gap, thus further lowering the energy of the  $0^+$  states. In relation to this last point, the shell model space above  $N = 50$  is also changed with respect to the case of  $^{90}\text{Zr}$ . Several recent studies have clearly shown that the  $\nu s_{1/2}$  shell drops in energy, becoming almost degenerate with the lower-lying  $\nu d_{5/2}$  shell at  $Z = 32$  and 30 [16,27]. As a consequence, neutron pair excitations across  $N = 50$  are likely to involve both orbits, leading to significant configuration mixing. The mechanism in this case is actually similar to the one determining the islands of inversion at  $N = 20$  in  $^{32}\text{Mg}$  [2] and at  $N = 40$  in  $^{64}\text{Cr}$  [28–30]. It appears that the common driving force that lowers the energy of intruder  $(2p - 2h)$  configurations is the quadrupole interaction in the quasi-SU(3) scheme [26,31], which involves  $\Delta J = \Delta \ell = 2$  orbitals. This scheme is realized for  $f_{7/2}p_{3/2}$  at  $N = 20$  [32] and for  $g_{9/2}d_{5/2}$  at  $N = 40$  and 50 [29,30]. Actually, the  $g_{9/2}d_{5/2}s_{1/2}$  space provides a paradigmatic example of the quasi-SU(3) scheme [29].

A quantitative description of the energy position of the  $0_2^+$  state requires knowledge of the evolution of two of the most important components of the nuclear Hamiltonian: the monopole and the quadrupole terms. In fact, the energy of the  $0_2^+$  level originating from a  $(2p - 2h)$  excitation can be expressed for  $N = 50$  as [33]

$$E_{0_2^+} = 2(E_{\nu d_{5/2}} - E_{\nu g_{9/2}}) + \Delta E_{\text{pair}}^{\nu\nu} + \Delta E_M^{\pi\nu} + \Delta E_Q^{\pi\nu},$$

where  $E_{\nu d_{5/2}} - E_{\nu g_{9/2}}$  is the energy difference between the unperturbed neutron states across  $N = 50$ . The unperturbed shell gap is then calculated as  $E_{\nu d_{5/2}} - E_{\nu g_{9/2}} = S_n(^{90}\text{Zr}) - S_n(^{91}\text{Zr})$ . The pairing term  $\Delta E_{\text{pair}}^{\nu\nu}$  was estimated using the one- and two-neutron separation energies and corresponds to the value  $[2S_n(^{90}\text{Zr}) - S_{2n}(^{90}\text{Zr})] + [2S_n(^{91}\text{Zr}) - S_{2n}(^{92}\text{Zr})]$  [34]. The neutron separation energies  $S_n$  are the ones evaluated in Ref. [35], which includes recent high-precision mass measurements [5,6].

The quadrupole  $\Delta E_Q^{\pi\nu}$  and the monopole  $\Delta E_M^{\pi\nu}$  contributions are the most interesting ones. The former was estimated using the IBM-2 approximation, following the prescriptions in Ref. [34].

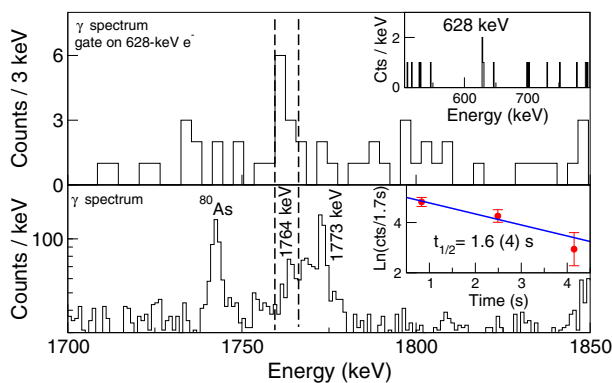


FIG. 3. Upper panel:  $\gamma$  spectrum gated on the 628 keV  $e^-$ . The peak at 1764 keV is clearly visible. The inset shows the inverse coincidence on the Si(Li) spectrum. Lower panel:  $\gamma$  spectrum,  $\beta$  gated, and enlarged in the region of interest. The inset shows the decay curve of the 1764 keV  $\gamma$  ray, compatible with the  $^{80}\text{Ga}$  lifetime(s).

The monopole energy difference was extracted from the discontinuity in the  $S_n$  curves across  $N = 50$  for each isotopic chain using the graphical method introduced in Ref. [36]. This enables us to extract a realistic  $\nu g_{9/2}\nu d_{5/2}$  gap. The obtained monopole energy slope is compatible with that of Ref. [37].

Figure 4 shows the evolution of the different contributions for the  $N = 48$  isotones, including the resulting energy of the intruder  $0_2^+$  level. The violet line is the pairing gain of the  $\nu(2p - 2h)$  configuration, with an error bar that represents the variation of pairing along the isotonic chain. The quadrupole contribution (orange line) has a minimum at  $Z = 34$ , at the  $f_{5/2}p_{1/2}p_{3/2}$  midshell, in accordance with the literature [38]. The quadrupole strength is consistent with estimates in this and other regions [1,25]. The monopole energy gain (red line) steadily increases as it approaches the Ge isotopes, and reduces slightly when going from the Ge to the Zn isotopes. The cumulative contribution of this gap reduction and the quadrupole gain in energy is the crucial factor that lowers the energy of the intruder configuration down to the measured value. The calculations thus show that the low energy of the  $0_2^+$  state cannot be explained only in terms of pairing and quadrupole correlations, but also demands a  $\sim 1$  MeV  $N = 50$  gap reduction. An error bar is added as a shaded area, and it reflects the uncertainties ( $\sim 300$  keV) in the mass evaluations [35] for  $^{83}\text{Zn}$ , since its mass has not yet been measured. The  $S_n$  of this nucleus is in fact necessary to apply the aforementioned graphical method. The resulting energy of the  $\nu(2p - 2h)$   $0_2^+$  states in  $N = 48$  isotones has a minimum in the  $Z = 32$  and  $34$  isotopes, as shown by the green line with its error bar coming from the pairing and the monopole contributions. Besides mass

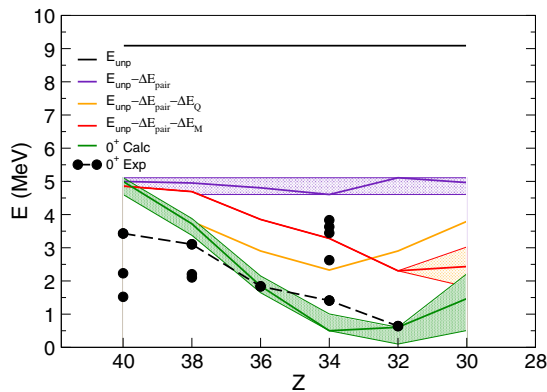


FIG. 4. Evolution of the different contributions for the  $N = 48$  isotones  $\nu(2p - 2h)$   $0_2^+$  states. The minimum of the excitation energy is flattened out towards  $Z = 32$  (Ge), due to the monopole drift. The pairing and monopole energy gains are given with an error bar, which contributes to the final error bar on the  $0_2^+$  state energy (see the text for details). The black dots are the known excited  $0_2^+$  states, and the ones best fitting the  $\nu(2p - 2h)$  configuration are linked by a dashed line to show the trend.

measurements, other studies have consistently pointed out the existence of this minimum of the  $N = 50$  shell gap, and the corresponding increase in collectivity [4,7,8]. It is not easy to establish the nature of  $0_x^+$  states over the whole isotonic chain, but it is observed that for each isotope there is at least one state with an energy compatible with the theoretical estimate for a  $(2p - 2h)$  intruder level. The exception of  $^{88}\text{Zr}$  may be linked to the imperfect closure of the  $Z = 40$  shell. The new  $0_2^+$  state found in the present work in  $^{80}\text{Ge}$  is compatible with the calculated range of values. It is thus tentatively interpreted as a  $\nu(2p - 2h)$  excitation across the  $N = 50$  shell closure. This  $\nu(2p - 2h)$  state has to be well deformed because of the quadrupole interaction between the valence nucleons. The presence of a deformed state near the almost spherical ground state, even lower than the first-excited  $2^+$  state, is an evidence of shape coexistence [12].

The 8.5-MeV lowering of the  $\nu(2p - 2h)$  configuration, from an unperturbed single-particle energy at  $\sim 9$  MeV to the measured 639 keV, is a remarkable effect of the quadrupole and monopole correlations in the nuclear Hamiltonian. Both provide an extra binding of  $\sim 2.5$  MeV at their maximum values at midshell  $Z = 34$  and at  $Z = 32$ , respectively, as shown in Fig. 4. The spherical shell-gap reduction induced by the monopole force has the effect to bring the minimum of the intruder configuration energy towards the lighter  $N = 50$  isotones. The lack of mass measurements in the most exotic isotopes prevents a precise prediction of the evolution towards  $^{78}\text{Ni}$ . If the monopole contribution does not increase the  $N = 50$  gap substantially from  $Z = 30$  to  $Z = 28$ , shape coexistence with a low  $\sim 2.5$  MeV intruder  $0_2^+$  state in  $^{78}\text{Ni}$  may occur. Moreover, a weakening of the  $Z = 28$  gap could further lower the  $\nu(2p - 2h)$   $0_2^+$  state via quadrupole interactions. Therefore, the evaluation of the spherical gap in  $^{78}\text{Ni}$  demands some caution. This is strictly correlated to the evolution of effective single-particle energies beyond  $N = 50$ : experimental evidence gathered so far is inexplicable using only two-body nuclear interactions [7]. The unequivocal determination of single-particle strengths, together with mass measurements of more exotic nuclei going towards  $^{78}\text{Ni}$ , are observables essential in the near future.

In summary, the present Letter shows the first clear evidence of shape coexistence in the  $N = 50$  neutron-rich region, by measuring a low-lying 639(1) keV  $0_2^+$  state in  $^{80}\text{Ge}$ , interpreted as a  $\nu(2p - 2h)$  excitation across  $N = 50$ . This finding is in agreement with phenomenological estimates from mass data, which point to a lowering of the intruder configuration as a result of monopole and quadrupole effects. The monopole contribution determines a reduction of the  $N = 50$  shell gap when going from  $Z = 40$  to  $Z = 32$ . This makes the  $Z = 34$  midshell correlation maximum flatten out towards  $Z = 32$ . These results suggest the possibility of shape coexistence in  $^{78}\text{Ni}$ . However, the lack of mass measurements of the most exotic

nuclei in this region hampers the precise assessment of the evolution of the  $N = 50$  shell gap and of the related effective single-particle energies down to  $Z = 28$ .

We thankfully acknowledge the work of the ALTO technical staff for the excellent operation of the ISOL source. We express our gratitude to ISOLDE Collaboration for having provided the ISOL target. We are grateful to E. Clement, F. Nowacki, and P. Sarriguren for fruitful discussions and to F. Azaiez for the careful reading of the Letter. C. A. acknowledges the support from the Natural Sciences and Engineering Research Council of Canada. Use of Ge detectors from the French-UK IN2P3-STFC Gamma Loan Pool is acknowledged.

*Note added.*—We recently became aware of the work in Ref. [39]. The authors measured the isomer shift of the  $1/2^+$  intruder state in the  $N = 49$   $^{79}\text{Zn}$  isotope. They found a large isomer shift with respect to the ground state, interpreted as an increased deformation. This result provides further evidence of the coexistence between a deformed low-energy intruder state and the normal-configuration ground state in this region.

---

\*gottardo@ipno.in2p3.fr

- [1] K. Heyde and J. L. Wood, *Rev. Mod. Phys.* **83**, 1467 (2011).  
 [2] E. K. Warburton, J. A. Becker, and B. A. Brown, *Phys. Rev. C* **41**, 1147 (1990).  
 [3] A. Bulgac and C. Lewenkopf, *Phys. Rev. Lett.* **71**, 4130 (1993).  
 [4] T. Rzaca-Urban, W. Urban, J. L. Durell, A. G. Smith, and I. Ahmad, *Phys. Rev. C* **76**, 027302 (2007).  
 [5] J. Hakala, S. Rahaman, V. V. Elomaa, T. Eronen, U. Hager, A. Jokinen, A. Kankainen, I. D. Moore, H. Penttila, S. Rinta-Antila, J. Rissanen, A. Saastamoinen, T. Sonoda, C. Weber, and J. Aysto, *Phys. Rev. Lett.* **101**, 052502 (2008).  
 [6] S. Baruah, G. Audi, K. Blaum, M. Dworschak, S. George, C. Guenaut, U. Hager, F. Herfurth, A. Herlert, A. Kellerbauer, H. J. Kluge, D. Lunney, H. Schatz, L. Schweikhard, and C. Yazidjian, *Phys. Rev. Lett.* **101**, 262501 (2008).  
 [7] K. Sieja and F. Nowacki, *Phys. Rev. C* **85**, 051301(R) (2012).  
 [8] M. Bender, G. F. Bertsch, and P.-H. Heenen, *Phys. Rev. C* **78**, 054312 (2008).  
 [9] A. P. Zuker, *Phys. Rev. Lett.* **90**, 042502 (2003).  
 [10] H. Morinaga, *Phys. Rev.* **101**, 254 (1956).  
 [11] N. Bree *et al.*, *Phys. Rev. Lett.* **112**, 162701 (2014).  
 [12] A. N. Andreyev *et al.*, *Nature (London)* **405**, 430 (2000).  
 [13] P. Hoff and B. Fogelberg, *Nucl. Phys.* **A368**, 210 (1981).  
 [14] R. A. Meyer, O. G. Lien, and E. A. Henry, *Phys. Rev. C* **25**, 682 (1982).  
 [15] A. Etile *et al.*, *Phys. Rev. C* **91**, 064317 (2015).  
 [16] R. Orlandi *et al.*, *Phys. Lett. B* **740**, 298 (2015).  
 [17] F. Ibrahim *et al.*, *Nucl. Phys.* **A787**, 110 (2007).  
 [18] S. Tusseau-Nenez *et al.*, *Nucl. Instrum. Methods Phys. Res., Sect. B* **370**, 19 (2016).  
 [19] D. Verney *et al.*, *Phys. Rev. C* **87**, 054307 (2013).  
 [20] T. Kibédi, T. W. Burrows, M. B. Trzhaskovskaya, P. M. Davidson, and C. W. Nestor, *Nucl. Instrum. Methods Phys. Res., Sect. A* **589**, 202 (2008).  
 [21] W. Schwerdtfeger, P. G. Thirolf, K. Wimmer, D. Habs, H. Mach, T. R. Rodriguez, V. Bildstein, J. L. Egido, L. M. Fraile, R. Gernhauser, R. Hertzenberger, K. Heyde, P. Hoff, H. Hubel, U. Koster, T. Kroll, R. Krucken, R. Lutter, T. Morgan, and P. Ring, *Phys. Rev. Lett.* **103**, 012501 (2009).  
 [22] A. C. Rester, J. H. Hamilton, A. V. Ramayya, and N. R. Johnson, *Nucl. Phys.* **A162**, 481 (1971).  
 [23] B. Fogelberg *et al.*, *Phys. Lett.* **37B**, 372 (1971).  
 [24] D. Burch, P. Russo, H. Swanson, and E. G. Adelberger, *Phys. Lett.* **40B**, 357 (1972).  
 [25] D. Pauwels, J. L. Wood, K. Heyde, M. Huyse, R. Julin, and P. Van Duppen, *Phys. Rev. C* **82**, 027304 (2010).  
 [26] E. Caurier, G. Martínez-Pinedo, F. Nowacki, A. Poves, and A. P. Zuker, *Rev. Mod. Phys.* **77**, 427 (2005).  
 [27] J. S. Thomas, G. Arbanas, D. W. Bardayan, J. C. Blackmon, J. A. Cizewski, D. J. Dean, R. P. Fitzgerald, U. Greife, C. J. Gross, M. S. Johnson, K. L. Jones, R. L. Kozub, J. F. Liang, R. J. Livesay, Z. Ma, B. H. Moazen, C. D. Nesaraja, D. Shapira, M. S. Smith, and D. W. Visser, *Phys. Rev. C* **76**, 044302 (2007).  
 [28] O. Sorlin *et al.*, *Eur. Phys. J. A* **16**, 55 (2003).  
 [29] S. M. Lenzi, F. Nowacki, A. Poves, and K. Sieja, *Phys. Rev. C* **82**, 054301 (2010).  
 [30] C. Santamaria *et al.*, *Phys. Rev. Lett.* **115**, 192501 (2015).  
 [31] A. P. Zuker, J. Retamosa, A. Poves, and E. Caurier, *Phys. Rev. C* **52**, R1741 (1995).  
 [32] K. Heyde and J. L. Wood, *J. Phys. G* **17**, 135 (1991).  
 [33] J. L. Wood, K. Heyde, W. Nazarewicz, M. Huyse, and P. van Duppen, *Phys. Rep.* **215**, 101 (1992).  
 [34] K. Heyde, J. Jolie, J. Moreau, J. Ryckebusch, M. Waroquier, P. Van Duppen, M. Huyse, and J. L. Wood, *Nucl. Phys.* **A466**, 189 (1987).  
 [35] M. Wang, G. Audi, A. H. Wapstra, F. G. Kondev, M. MacCormick, X. Xu, and B. Pfeiffer, *Chin. Phys. C* **36**, 1603 (2012).  
 [36] K. Heyde, J. Jolie, J. Moreau, J. Ryckebusch, M. Waroquier, and J. L. Wood, *Phys. Lett. B* **176**, 255 (1986).  
 [37] M.-G. Porquet and O. Sorlin, *Phys. Rev. C* **85**, 014307 (2012).  
 [38] M. Dufour and A. P. Zuker, *Phys. Rev. C* **54**, 1641 (1996).  
 [39] X. F. Yang *et al.*, following Letter, *Phys. Rev. Lett.* **116**, 182502 (2016).